Published by

British Journal of Contemporary Research

BEXFORD PUBLISHING

Spectral Discrimination of Ground Level Enhancements and Magnetospheric Effects Using Energy-Resolved Muon and Neutron Measurements from the SEVAN Light Detector Network

Original Research Article | Volume 1 | Issue 3 | 2026 | Article Number: 008

Accepted: 21 July 2026 | Published: 10 August 2026 | ISSN: 2979-8582 (Online)

Crossref : **https://doi.org/10.67693/BJCR-M77CHXH8**

Ashish Kumar Meena

Visiting Faculty, Poornima University, Jaipur, Rajasthan, India

AKM [0000-0002-1674-0252](0000-0002-1674-0252)

Correspondence: Ashish Kumar Meena, ashishmeena944@gmail.com

Abstract

Simultaneous enhancements of neutron and muon fluxes, driven either by solar energetic particles or by magnetospheric disturbances, offer a valuable window into solar modulation processes and into the physical mechanisms behind space-weather events. This paper describes an extended capability of the SEVAN light detector network, which records full energy-release histograms of secondary particles rather than the flux-only counts provided by conventional cosmic-ray monitors. Using data acquired at the Aragats (Armenia) and Zugspitze (Germany) stations, we contrast the energy-release signatures of a Ground Level Enhancement, GLE #74 of 11 May 2024, with those of a Magnetospheric Enhancement (ME) recorded on 5 November 2023. The GLE event produced broad energy-release spectra reaching well beyond 100 MeV, consistent with the arrival of relativistic solar protons, whereas the ME event remained confined almost entirely below 10 MeV, a signature of its magnetospheric rather than solar origin. This spectral contrast provides a practical means of separating solar from magnetospheric contributions to ground-level particle counts, while also placing approximate constraints on the primary particle energies responsible for the observed secondary cascades. The method strengthens the diagnostic reach of ground-based detector networks for event classification and contributes to improved forecasting of space-weather conditions.

Keywords: Ground Level Enhancements, Magnetospheric Enhancements, Sevan Light Detector, Neutron And Muon Spectroscopy, Solar Energetic Particles, Space Weather

1. Introduction

Ground-based particle detector networks remain one of the most direct ways of tracking the response of the terrestrial atmosphere to variable solar and magnetospheric activity. Among these networks, the SEVAN (Space Environmental Viewing and Analysis Network) light detectors installed at the Aragats and Zugspitze mountain stations have repeatedly demonstrated their usefulness for identifying Ground Level Enhancements (GLEs), Magnetospheric Effects, and Forbush decreases (FDs) in near real time.

A distinguishing feature of the SEVAN instrument is that it is a compact and relatively inexpensive particle detector capable of recording, simultaneously, both the count rate and the energy deposited by charged and neutral secondary cosmic-ray particles. Few other detector types offer this dual capability (1). This design makes it particularly well suited to the study of several related atmospheric and space-weather phenomena:

- Thunderstorm Ground Enhancements (TGEs), where energy-resolved measurements assist in reconstructing the electron and gamma-ray spectra produced during thunderstorms;
- Solar Energetic Particle (SEP) events and Ground Level Enhancements (GLEs), in which the enhancement of secondary muons and neutrons carries information about the energy of the primary solar protons;
- Forbush decreases (FDs), detected through the precise measurement of transient depressions in cosmic-ray flux;
- Magnetospheric Effects (MEs), which arise from geomagnetic modulation of low-energy muon and neutron fluxes.

The present study builds on this capability to examine, in a comparative and quantitative way, how energy-release histograms differ between a genuine solar GLE and a magnetospheric enhancement, using two representative events recorded during 2023-2024(2-3).

2. Instrumentation and Methodology

Energy-release histograms were compared using plastic scintillators of different thickness at the two stations: a 20 cm thick, 0.25 m² spectrometric scintillator at Aragats, and a 25 cm thick scintillator of the same footprint at Zugspitze(4-5). Each spectrometric scintillator is shielded from above by a veto scintillator of 1 m² area, 1 cm thick at Aragats and 5 cm thick at Zugspitze, used to reject particles that do not fully deposit their energy within the spectrometer volume. Both stations use identical data-acquisition electronics, with linear amplitude-to-digital converters (LADCs) covering an energy-release range of up to 300 MeV(6-7).

Each energy-release histogram consists of excess counts above background, sorted into 128 energy bins. Background spectra were obtained from fair-weather periods preceding each solar or magnetospheric event, and were subtracted from the event-time histograms to isolate the enhancement associated with the event itself (8).

Table 1 summarises the two events examined in this work, together with the hourly count excess recorded at maximum intensity at each site. The peak GLE flux occurred between 02:30 and 03:30 UT on 11 May 2024, while the peak ME flux occurred between 11:00 and 12:00 UT on 5 November 2023(9). As shown in the table, several thousand excess particles were registered per hour at both stations for both events, a statistic large enough to support a reliable spectral classification of the two phenomena.

Date	Location	Rc (GV)	Particle Type	Primary Type	Primary Energy (GeV)	Hourly Excess
11 May 2024	Zugspitze	3.7	Muons	SCR	8–10	10426
11 May 2024	Zugspitze	3.7	Neutrons	SCR	8–10	11232
5 Nov 2023	Zugspitze	3.7	All particles	GCR	3.6	4658
11 May 2024	Aragats	7.1	Muons	SCR	8–10	7190
11 May 2024	Aragats	7.1	Neutrons	SCR	8–10	9631
5 Nov 2023	Aragats	7.1	All particles	GCR	7.0	4102

Table 1. Summary of muon and neutron energy-release statistics for the GLE of 11 May 2024 and the ME of 5 November 2023.

At Zugspitze, the combined hourly excess of muons and neutrons during the GLE exceeded 21,000 counts, indicative of a strong injection of relativistic solar protons. Aragats, despite its higher geomagnetic cutoff rigidity (Rc = 7.1 GV), still registered more than 16,000 excess counts, confirming that solar cosmic rays of sufficiently high energy penetrated even this more strongly shielded site. At both stations the neutron excess exceeded the muon excess, consistent with efficient hadronic cascade development. By contrast, the hourly excess during the ME event was only 4,100–4,600 counts at the two stations, roughly a factor of four below the GLE values. This reduction reflects the comparatively low energy of the galactic cosmic-ray protons responsible for the ME, which lie below the local geomagnetic cutoff and only reach the middle atmosphere through magnetospheric modulation rather than direct atmospheric penetration. The shape of the corresponding histograms (discussed in Section 3.2) further supports this interpretation, since no high-multiplicity muon or neutron signature is present in the ME data[10].

This four-fold contrast in event intensity, together with the differing histogram shapes, illustrates how SEVAN energy-release data can be used to:

- Distinguish solar from magnetospheric contributions to a given enhancement;
- Estimate the approximate energy and spectral shape of the primary SEP population; and
- Support atmospheric shower simulations (e.g., with CORSIKA) by comparing observed energy-release histograms with those expected for monoenergetic primary protons.

Taken together, these capabilities extend the usefulness of ground-based SEVAN monitoring for both solar event research and operational space-weather diagnostics.

3. Results

3.1 Detection of GLE #74 at Mid-Latitude Neutron Monitor and SEVAN Stations

The G5-class geomagnetic storm of 10–11 May 2024 ranks among the strongest of the past two decades (Hayakawa et al., 2024). The storm was accompanied by a pronounced Forbush decrease, followed during its recovery phase by GLE #74. Both the global neutron monitor network and the SEVAN stations recorded a GLE onset near 02:00 UT on 11 May 2024, roughly half an hour after the peak of an X5.8 solar flare at 01:23 UT. Standard neutron-monitor classification initially assigned a "zero response" to all non-polar stations, since the GLE onset coincided with the early recovery phase of the FD, making the two signals difficult to separate using count rate alone.

At both Aragats and Lomnicky Štít, however, the combination of neutron monitor and SEVAN measurements made it possible to resolve the two signals. Figure 1 shows the FD recovery trend (dashed blue line) together with the Lomnicky Štít neutron monitor time series (blue) and the corresponding SEVAN count rate (green), with the GLE enhancement highlighted as a shaded blue region. The two independent instruments trace essentially the same enhancement superimposed on the underlying FD recovery, confirming that the GLE signal was real rather than an artefact of the recovering count rate.

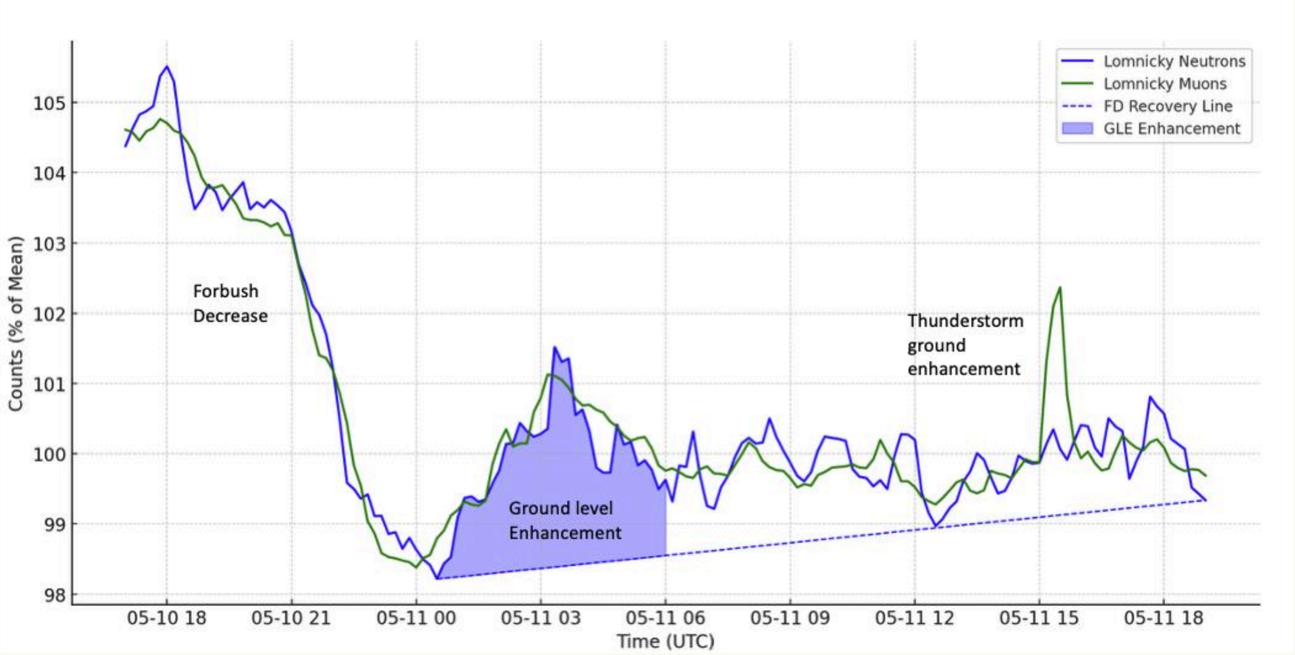

Figure 1. Forbush decrease and GLE #74 as recorded by the Lomnicky Štít neutron monitor (blue) and the upper 5 cm SEVAN scintillator (green). The dashed line marks the FD recovery trend; the shaded region marks the GLE enhancement.

A second, unrelated enhancement is visible in the SEVAN count rate near 15:00 UT on the same day. This later peak is attributed to a Thunderstorm Ground Enhancement, produced by bursts of electrons and gamma rays generated in runaway-electron avalanches within a locally disturbed atmosphere. Its presence is a useful reminder that reliable GLE identification also requires monitoring of local atmospheric conditions — temperature, pressure, and electric field — since these can independently modulate the count rate.

Figure 2 presents the equivalent comparison at Aragats, combining the Aragats neutron monitor (red) with the SEVAN neutron (blue) and muon (green) channels. As at Lomnicky Štít, the FD recovery trend is marked with a dashed line and the GLE enhancement with a shaded region. The GLE is again registered simultaneously by both instrument types, with a time profile closely resembling that seen at Lomnicky Štít, giving an independent, two-station, two-detector-type confirmation of the same solar event.

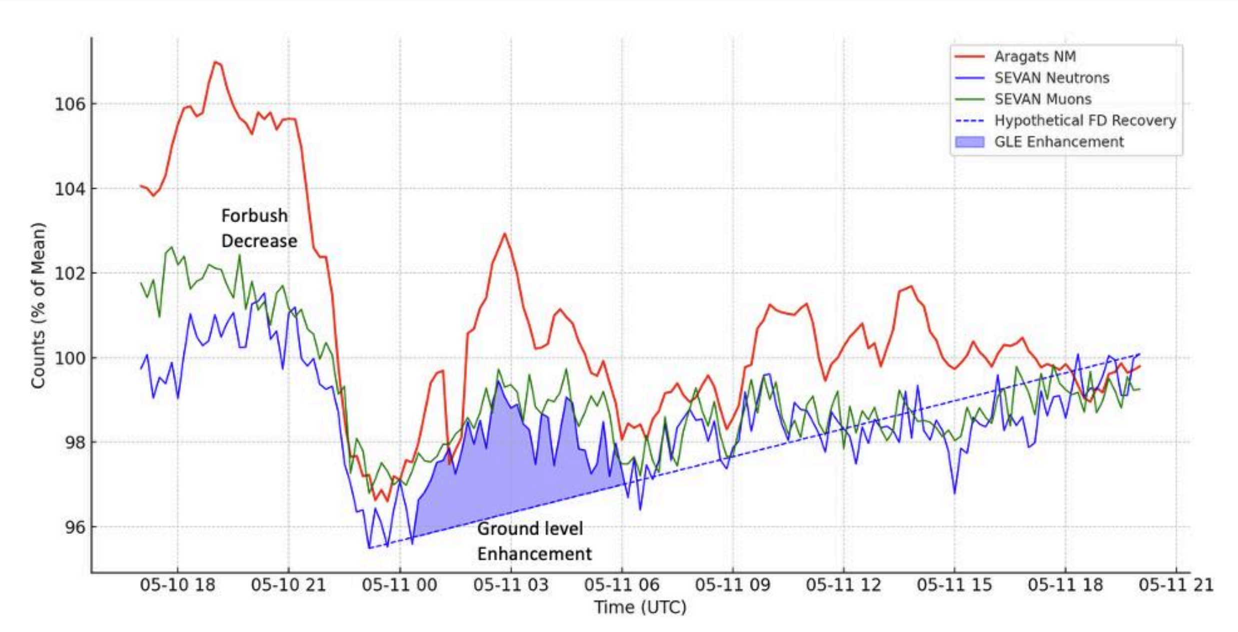

Figure 2. Forbush decrease and GLE #74 as recorded by the Aragats neutron monitor (red) and the SEVAN light detector, neutron channel (blue) and muon channel (green).

Figure 3 shows local atmospheric conditions during the same interval — outside temperature (red) and atmospheric pressure (green) — together with the count-rate time series of the Aragats Solar Neutron Telescope (blue), an instrument designed to search for neutrons emitted directly from the flare site. Both temperature and pressure remained relatively stable through the FD and GLE period, indicating that atmospheric effects were not the dominant driver of the observed count-rate variations. A second, smaller flux increase visible after the main GLE peak is attributed instead to a modest depletion of atmospheric pressure.

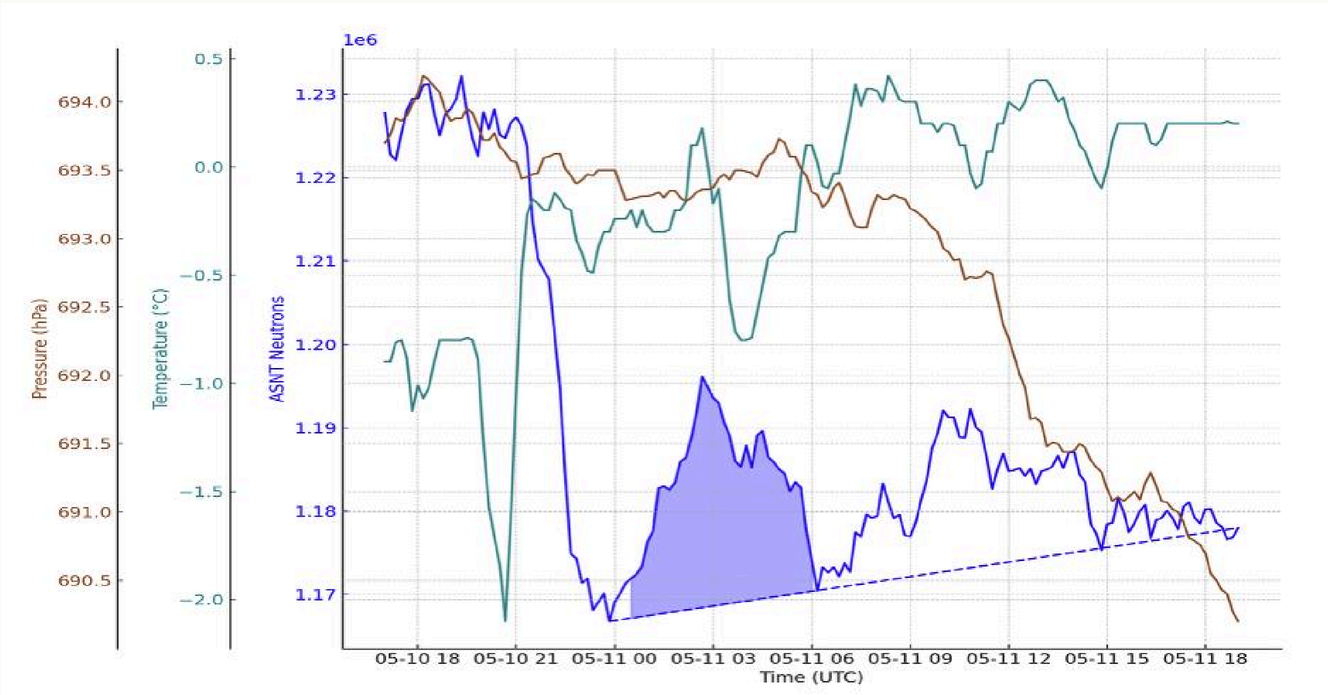

Figure 3. Aragats Solar Neutron Telescope count rate (blue) alongside outside temperature (green) and atmospheric pressure (red). The dashed line marks the FD recovery trend; the shaded region marks the GLE enhancement.

Taken together, Figures 1–3 demonstrate that the GLE was genuinely registered at mid-latitude stations, and was not simply an artefact of the rising FD recovery phase. Multiple independent detectors, at two separate sites, consistently show the same enhancement superimposed on the FD recovery trend.

3.2 Energy-Release Histograms for the GLE and ME Events

Figure 4 shows the neutron and muon energy-release histograms recorded simultaneously at Aragats (Rc = 7.1 GV) and Zugspitze (Rc = 3.7 GV) during the peak hour of GLE #74, 02:30–03:30 UT on 11 May 2024. Panel (a) shows the Aragats muon spectrum, subdivided into electrons (0–25 MeV, black), single muons (25–60 MeV, blue), double muons (60–100 MeV, red), and multiple-muon events (>100 MeV, green). Panel (b) gives the corresponding Aragats neutron spectrum, dominated by evaporation neutrons below 50 MeV. Panels (c) and (d) show the analogous muon and neutron spectra at Zugspitze; here the muon spectrum is shifted markedly toward higher energies, with a pronounced peak in the 100–250 MeV range reflecting a larger number of multiple-muon events, while the neutron spectrum remains, as at Aragats, dominated by sub-50 MeV evaporation neutrons.

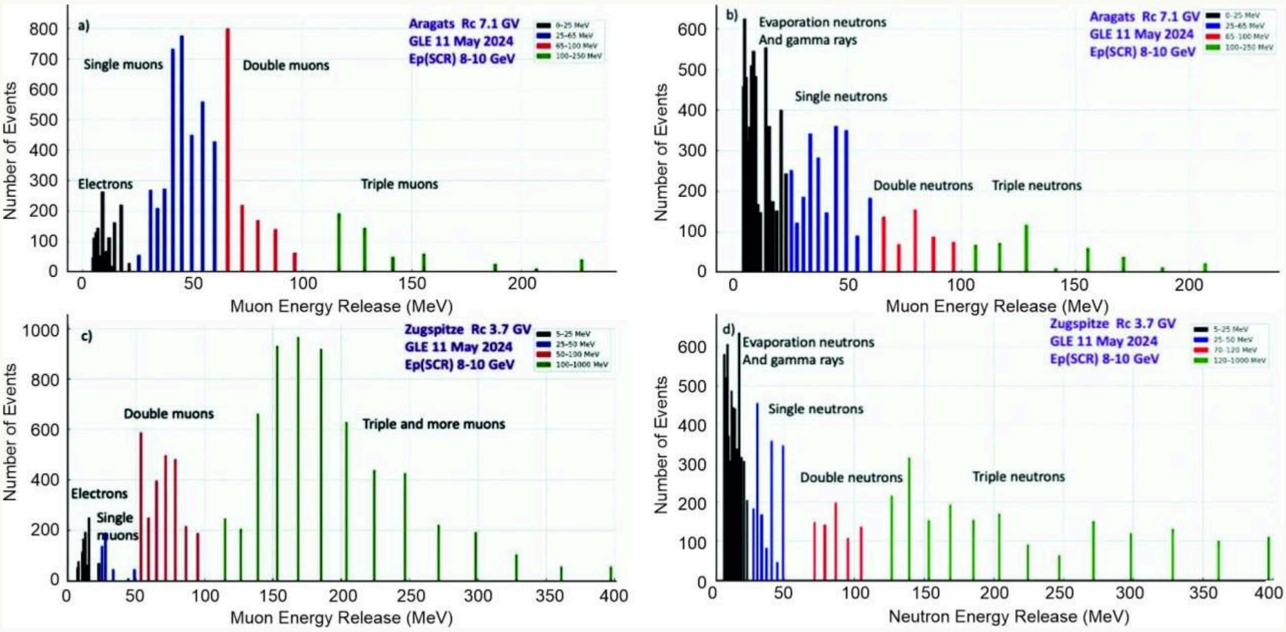

Figure 4. Energy-release histograms of muons and neutrons recorded by the SEVAN light detector at Aragats (a, b) and Zugspitze (c, d) during GLE #74.

The muon histograms resolve single, double, and multiple coincidences considerably more clearly than the neutron histograms do. Model calculations indicate that the contribution of low-energy muons to the lowest energy bins is negligible, so particles registered below 25 MeV in the charged ("11") coincidence channel are predominantly electrons. The 25–60 MeV band reflects a mixture of electrons and low-energy muons crossing the scintillator at varying angles, given that muon energy loss in the scintillator is of the order of 2 MeV per centimetre. The 60–100 MeV band is attributable mainly to double-muon events or to more complex interactions of high-energy muons within the spectrometer, while the region above 100 MeV corresponds to muon bundles or further high-energy muon interactions. This multiplicity separation is possible because of the well-defined energy loss of minimum-ionizing muons, the wide dynamic range of the spectrometer, and the 1 ms coincidence window used to reject accidental coincidences and diffuse background. The neutral ("01") channel, by contrast, is affected by larger timing uncertainties, energy-dependent moderation, and overlapping thermal-capture signals, which together smear the neutron histogram and make multiplicities harder to resolve. This contrast highlights the particular value of muon spectrometry for probing the high-energy structure of secondary particle production during GLEs, and for linking the observed energy-release pattern back to the primary proton energy.

The four panels of Figure 4 together illustrate a systematic contrast between muon and neutron energy-release signatures: the muon spectra (panels a, c) are broader and extend to higher energies, especially at Zugspitze, reflecting the cascading nature of the atmospheric shower, whereas the neutron spectra (panels b, d) remain sharply peaked at low energies, consistent with nuclear evaporation followed by rapid thermalisation.

The site-to-site differences seen in Figure 4 can be traced to the combined effects of geomagnetic cutoff rigidity, atmospheric depth, and detector geometry. At Zugspitze (Rc = 3.7 GV, 2650 m altitude) a substantially larger flux of GeV-range protons can access the atmosphere than at Aragats (Rc = 7.1 GV, 3200 m altitude), which accounts for the pronounced high-energy tail and multiple-muon peak in the Zugspitze muon spectrum (Fig. 4c) relative to the more modest 25–100 MeV-dominated Aragats spectrum (Fig. 4a). A similar pattern appears in the neutron spectra: Zugspitze shows a longer high-energy tail extending toward 200–300 MeV (Fig. 4d), whereas the Aragats neutron spectrum falls off more steeply beyond about 100 MeV (Fig. 4b). Beyond the cutoff-rigidity effect, the greater atmospheric depth above Zugspitze (~730 g/cm²) compared with Aragats (~690 g/cm²) allows more extensive hadronic cascade development, increasing the likelihood that secondary muons and neutrons reach the ground with higher residual energy. The greater scintillator thickness at Zugspitze (25 cm versus 20 cm at Aragats) further raises the probability of full energy deposition for higher-energy secondaries. The combined effect of these three factors — cutoff rigidity, atmospheric depth, and scintillator thickness — explains why the Zugspitze energy-release spectra extend further and contain more high-multiplicity events than those recorded at Aragats.

Figure 5 shows the energy-release histograms recorded during the 5 November 2023 ME event at Aragats (a) and Zugspitze (b); particle-type discrimination was not yet available at the time of this event, so the histograms include all detected particles combined. In both cases, the distribution is narrow and approximately bell-shaped, confined between roughly 5 and 11 MeV and centred near 8–9 MeV, with no discernible high-energy tail. This is in clear contrast to the structured, multi-component muon histograms of the May 2024 GLE: no multiplicity groups are evident, and essentially no secondary particles exceed 20 MeV.

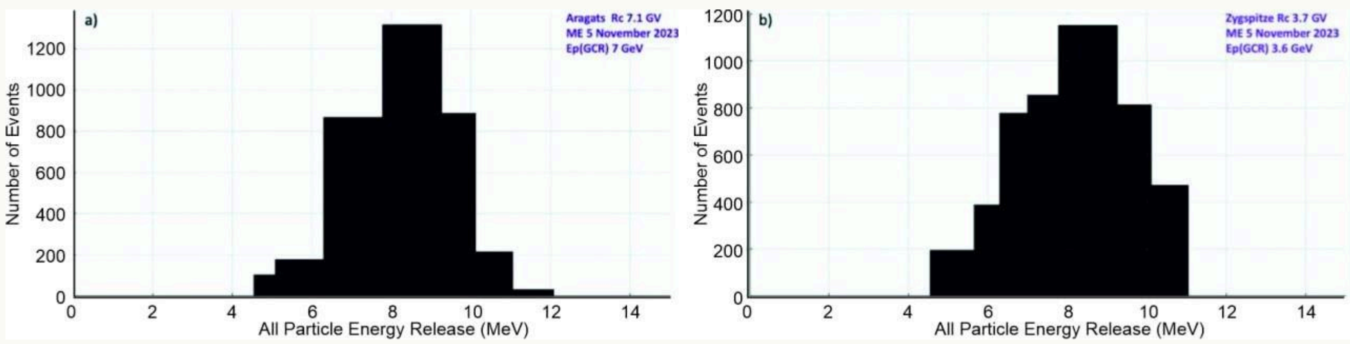

Figure 5. Energy-release histograms of all detected particles recorded by the SEVAN light detector at Aragats (a) and Zugspitze (b) during the ME event of 5 November 2023.

The expected primary proton energies for a magnetospheric event of this kind — that is, galactic cosmic-ray protons with energies just below the local geomagnetic cutoff — fall slightly under 7.1 GeV at Aragats and 3.7 GeV at Zugspitze. Under quiet magnetospheric conditions such sub-cutoff protons would not normally reach the atmosphere. The comparatively low energies seen in the observed histograms, well below those of the GLE event, are consistent with a magnetospheric effect in which an approaching coronal mass ejection temporarily perturbs the geomagnetic field, allowing sub-cutoff protons to penetrate into the middle atmosphere.

Relative to the May 2024 GLE, whose muon and neutron spectra extended well above 100 MeV with clear multiplicity structure, the November 2023 event is far more limited in both intensity and spectral hardness. The narrow, low-energy histogram shape is consistent with a population of soft secondaries — low-energy electrons, photons, and evaporation neutrons — generated by weak atmospheric cascades or sub-threshold interactions, and this soft-secondary signature is common to both stations.

The close similarity of the Aragats and Zugspitze spectra during this event is itself informative, pointing to a large-scale magnetospheric disturbance that:

- Partially suppressed the usual geomagnetic rigidity filtering;
- Produced only soft, low-energy secondary particles; and
- Generated closely matching spectral shapes at both stations, despite their differing cutoff rigidities.

These features support the interpretation of the 5 November 2023 event as a magnetospheric disturbance, physically distinct from a conventional high-energy solar proton event.

4. Discussion

The combined neutron-monitor and SEVAN record clearly establishes the presence of GLE #74 at mid-latitude stations on 11 May 2024. The underlying FD recovery, while present, was not the dominant driver of the observed count-rate enhancement, and the count rate did not return to its pre-storm baseline until roughly two days after the FD onset.

The absence of any high-energy tail in the 5 November 2023 event clearly separates it from a genuine solar GLE such as that of 11 May 2024. Considered together, the two events demonstrate how energy-resolved neutron and muon spectroscopy can be used to distinguish solar from geomagnetic sources of secondary-particle enhancement — a distinction that is difficult to make from flux data alone.

The parallel behaviour of the neutron-monitor and SEVAN records at Lomnicky Štít and Aragats confirms that the GLE enhancement and the FD recovery, though temporally overlapping, can be reliably deconvolved, and that the May 2024 GLE was genuinely observed at mid-latitude, as shown in Figures 1 and 2.

Comparing the 11 May 2024 GLE with the 5 November 2023 ME reveals a marked divergence in the energy content of the secondary particles reaching ground level. The GLE, driven by relativistic solar protons, is characterised by:

- Deeply penetrating particle showers;
- Clearly resolved muon and neutron multiplicities; and
- A wide energy-release spectrum spanning roughly 0–300 mev.

The me, by contrast, is characterised by:

- Low-energy, soft secondary particles;
- The absence of muon bundles or a hard neutron component; and
- A narrow, symmetric histogram centred near 8–9 mev.

Physically, the ME event reflects a temporary reduction in effective geomagnetic cutoff rigidity, which allowed galactic protons with energies below the nominal cutoff to reach the atmosphere and produce a modest secondary-particle excess at both stations. The GLE, in contrast, produced broad and structured spectra with distinct multiple-muon bands and a neutron tail extending well beyond 100 MeV —

signatures of relativistic secondaries generated by solar protons with primary energies clearly above the local cutoff, plausibly in the region of 8–10 GeV. The absence of high-energy muons and of multiplicity structure is therefore a reliable marker separating sub-cutoff magnetospheric events from super-cutoff solar GLEs.

A further, forward-looking application of this method is the comparison of SEVAN energy-release data with CORSIKA simulations of monoenergetic primary protons entering the atmosphere. Such a comparison offers a route to inferring the most probable primary SEP energy from the observed secondary spectrum — an inverse-modelling approach that could, in principle, support near-real-time assessment of solar proton events.

5. Conclusions

This study has shown that energy-resolved neutron and muon measurements from the SEVAN light detector network provide a practical and reliable way of distinguishing Ground Level Enhancements from Magnetospheric Enhancements. GLE #74 (11 May 2024), examined jointly with neutron-monitor data at Lomnicky Štít and Aragats, showed a broad energy-release spectrum extending beyond 100 MeV together with a clear muon and neutron multiplicity structure signatures of relativistic solar protons penetrating the atmosphere. The Magnetospheric Enhancement of 5 November 2023, by contrast, produced a narrow, low-energy histogram confined below about 10 MeV at both Aragats and Zugspitze, consistent with sub-cutoff galactic protons admitted by a temporarily weakened geomagnetic shield. Because these two classes of event leave clearly distinguishable spectral fingerprints, the approach described here offers ground-based detector networks an additional, complementary tool for event classification, for constraining primary particle energies, and ultimately for improving space-weather forecasting.

Data Availability Statement

SEVAN light detector data used in this study are available from the Aragats and Zugspitze station archives upon reasonable request to the corresponding author. Supporting solar flare and geomagnetic index data were obtained from the NOAA National Centers for Environmental Information (NCEI) and from NASA's Planetary Data System (PDS) space physics archives.

Declaration of Conflict of Interest

The author declares no conflict of interest.

Funding Information

This research received no external funding.

Author Contribution Statement

Ashish Kumar Meena: Conceptualization, Data curation, Formal analysis, Investigation, Methodology, Writing – original draft.

References

Gour, P. S., Meena, A. K., Verma, P. L., Soni, S., Sharma, J., & Yadav, V. (2024). Correlation analysis of key parameters associated with solar activity and geomagnetic disturbances throughout 2023. European Academic Research, 11(12), 1494–1504.

Mauthiya, N., Saini, S., & Meena, A. K. (2026). An analysis of the contribution of khadi and village industries in employment generation in Rajasthan. World Journal of Advanced Research and Reviews, 30(2), 2050–2060.

Meena, M. K., Meena, A. K., & Gour, P. S. (2022). Analysis of coronal mass ejections and solar flares. International Journal of Innovative Research and Growth, 11, 70–73.

Meena, A. K., & Gour, P. S. (2024). Investigating Asia's low latitude ionosphere's pulse during the spectacular September 2017 solar storms. Tuijin Jishu/Journal of Propulsion Technology, 45(1), 3322–3334.

Meena, A. K., Sharma, A., & Gour, P. S. (2024). Ionospheric responses to solar flares: An analysis of ion composition changes during moderately high solar activity in January 2023. World Journal of Advanced Research and Reviews, 21(3), 219–224.

Meena, A. K., Sharma, A., & Gour, P. S. (2024). The impact of moderate solar flare activity on ionospheric response from August 5th to 7th, 2023. World Journal of Advanced Research and Reviews, 22(1), 043–054.

Meena, A. K., Gour, P. S., & Soni, S. (2024). The effects of strong and weak solar flares on the total electron content in the ionosphere during the 2011 solar peak. African Journal of Biomedical Research, 27(4s), 2422–2433.

Prajapati, S. R., Pathak, K., Shrivastava, P., & Meena, A. K. (2025). Dengue in South Asia: Emerging epidemiological patterns and surveillance obstacles. Magna Scientia Advanced Biology and Pharmacy, 14(2), 91–114.

Tak, S. B., Godha, M., & Meena, A. K. (2025). Reproductive toxicity of microplastics: Role of oxidative stress in cellular and molecular damage. World Journal of Advanced Research and Reviews, 25(3), 203–213.

Vaswani, L. K., Gour, P. S., Meena, A. K., & Soni, S. (2022). Geomagnetic storm in association with solar activities. International Journal of Innovative Research and Growth, 11, 143–148.